Electrohydrodynamic Patterning of Thin Polymer Film

Ning Wu, Leonard F. Pease III, and William B. Russel

Department of Chemical Engineering, Princeton University,
Princeton, New Jersey 08544-5263, USA, nwu@princeton.edu

ABSTRACT

The polymer melt confined within two planner electrodes can self assemble into ordered structures under the influence of an electric field. Motivated by the variety of patterns observed in experiments for polymers under both unpatterned and patterned masks, we describe here, from the theoretical and numerical analyses, how the weakly and fully nonlinear effects govern the growth of the instability and determine the final patterns. In the second part of our manuscript, we show that the insights gained from the above theoretical and numerical studies can greatly help design "smart mask" to produce large scale alignment of ordered patterns over regions much greater in extent than their natural domain size. This first step in enabling engineering of electrohydrodynamic patterning over large areas opens the path towards applications requiring larger areas of well-arrayed patterning.

Keywords: electrohydrodynamic, patterning, thin polymer film

1 INTRODUCTION

In 1999 and 2000 the laboratories of Chou [1] and Russell [2] employed electrical forces to pattern thin, polymeric films into a wide variety of microstructures including discrete pillars and continuous ridges. Their processes begin by spin coating a thin polymer film onto a rigid substrate. A mask is then brought into close proximity with the film leaving an air gap. Under the influence of an internally built-up or externally applied electric field, the free interface between the polymer and air can deform and assemble into ordered microstructures when it is heated above the glass transition temperature of the film. The competition between electrical forces and surface tension sets a characteristic and periodic length for which perturbation to the film surface grows the fastest. Subsequent cooling the film to room temperature freezes the micron-sized structures, which can be observed by removing the mask mechanically.

Linear models [3,4] have successfully predicted that the most unstable wavelength λ_{max} ($\lambda_{max} = 2\pi / k_{max}$), which is close to the final pillar-to-pillar spacing, is proportional to square root of the interfacial tension γ and inversely proportional to the potential difference U between the mask and substrate. Nevertheless, the validity of the linear theory becomes questionable when the unstable disturbances reach appreciable amplitudes. Experimentally, one observes most often hexagonal arrays under unpatterned masks. Why does the hexagonal pattern seem to be the intrinsic pattern? This important question cannot be answered by a linear analysis, and the nonlinear terms must be taken into account if the spatial pattern or the long-time behavior of the growing disturbance is to be ascertained. Here, we perform a weakly nonlinear analysis and show that the second and third order nonlinearities favor the growth of hexagonal patterns under a featureless mask, in agreement with experimental observations.

The patterning induced by the electrohydrodynamic instability provides a convenient and cost-effective way to create small features on polymer or in the substrate without the need of expensive patterned masks, toxic chemicals, or exposure to light. However, the spatial ordering of the pattern is generally very hard to extend over large areas. Domain boundaries and defects anneal slowly, if at all. Under unpatterned masks, the hexagonally packed domains typically span about ten to fifteen pillars, or almost randomly on the substrate. Using patterned masks can guide the polymer into structures that conform completely to the pattern on the mask, i.e., a positive replication of the mask patterns. Nonetheless, replication requires an accurately patterned mask with all the desired features, which can be time-consuming and expensive especially with numerous and tiny features. To take full advantage of the capability of the electrohydrodynamic patterning under featureless masks and retain the goal of creating ordered patterns over large areas, we propose here a strategy of arranging relatively simple patterns on the mask to guide and align the growth of pillars into ordered patterns over spans much larger than previously achieved. Since the electrohydrodynamic force involved in this patterning is universal and non-material specific, the ability to assemble thin polymer films into ordered pattern over large areas should facilitate various applications of this technology, including fabrications of micro-electro-mechanical systems, chemical or biological sensors, optoelectronic devices, etc.

2 WEAKLY NONLINEAR ANALYSIS

The patterning of a thin polymer film via the electrohydrodynamic instabilities can be modeled as a Poiseuille's flow with the lubrication approximation and the evolution equation can be written as the following:

$$\frac{\partial h}{\partial t} = \nabla\left(\frac{1}{3\mu} h^3 \nabla p\right)$$
$$p = p_0 - \frac{U^2 \varepsilon_0 (\varepsilon - 1)\varepsilon}{2\left[h + (H-h)\varepsilon\right]^2} - \gamma \nabla^2 h + \left[\frac{A}{(H-h)^3} - \frac{A}{h^3}\right] \quad [1]$$

Here, we perform an analysis following the evolution of the axisymmetric and linearly unstable waves into the weakly nonlinear regime. This approach is similar to that developed by Fermigier et. al. for the Rayleigh-Taylor instability of a thin layer [5]. We select modes with particular wavelengths and orientations in the weakly nonlinear analysis based on the following assumptions: (1) the modes with the largest growth rate in the linear theory will dominate others as long as the amplitude of disturbance is small. Therefore those wave vectors amplitudes of $k_{\max}$ should be selected. (2) The specific orientations of these most unstable waves should be consistent with the final patterns of, e.g., stripes, squares, and hexagons. Therefore, we will choose one, two, or three pairs of wave vectors to represent each pattern. (3) Harmonic modes with $\mathbf{k} = 2\mathbf{k_i}$ and resonant modes with $\mathbf{k} = \mathbf{k_i} - \mathbf{k_{i+1}}$ are also included, because they are regenerated continuously through the nonlinear interactions among the most unstable modes.

We assume the order of magnitudes of the most unstable modes in the linear growth regime to be β, the nonlinear interactions between $\mathbf{k_i}$ and $\mathbf{k_j}$ generate harmonic and resonant modes with amplitudes of order β^2. In turn, these newly generated modes interact with the main modes $\mathbf{k_i}$ and $-\mathbf{k_i}$ to modify the growth of amplitudes at order β^3, which is the minimum order that must be included for stripe, square, and hexagonal patterns in the weakly nonlinear regimes. We omit tedious algebra here and plot the variation of $\ln[A_u(t)/A_u(0)]$ for four different patterns: the stripe, square, hexagonal-pillars, and hexagonal-holes with a typical value of h_0 and ε in Fig. 1 [6]. The linear growth is also included for comparison. At early time, i.e. for small disturbances, all patterns grow linearly. As the amplitude of instability grows, the hexagonal-peaks pattern outpaces the others because of the interactions between different modes. Our investigations over a fairly wide range of h_0 h_0 ($0 < h_0 < 0.8$) and ε ($1 < \varepsilon < 10$) show that, compared with the stripe and square pattern, the hexagonal-pillars is dominant for growth under unpatterned masks. This agrees with the experimental observations for polymer-air systems and is confirmed by the numerical simulations as shown elsewhere. Also from Fig. 1, the stripe instability grows the slowest and even decays when the initial film thickness is small. The nonlinear interactions tend to damp the growth of stripe pattern, which makes it particularly difficult to observe in experiments.

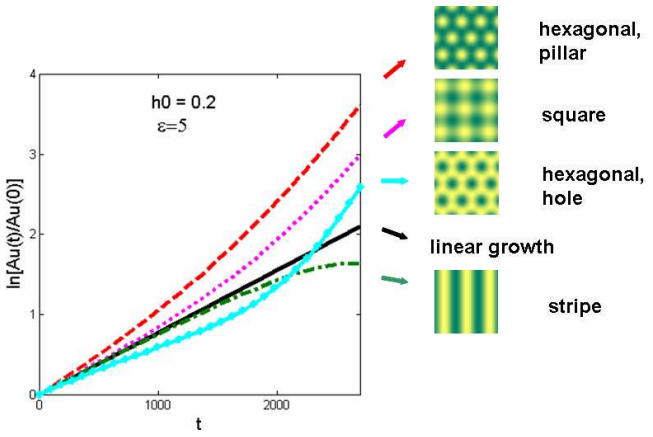

Figure. 1 Evolution of the amplitudes of main modes for different patterns (polymer-air system under a featureless mask).

Our numerical study shows that if the dielectric constant ratio of the upper layer is larger than the bottom one, a two-dimensional hole structure can be formed, in agreement with experimental observations [7]. These intriguing arrays raise a question that why holes form instead of pillars under these conditions. This differentiation can be understood qualitatively within the context of the weakly nonlinear theory. If we constrain ourselves temporarily to the two-dimensional hexagonal patterns of pillars and holes, the governing equation to third order in the amplitude A of the three pairs of primary modes that constitute a hexagonal pattern can be written as

$$\frac{dA}{dt} = \alpha A + \xi A^2 + \kappa A^3 \quad [2]$$

where α, ξ, and κ are the coefficients associated with different orders of A and depend on the system parameters. The hexagonal pillar and hole patterns are distinguished by the amplitude reflection $A \to -A$. For a positive (negative) ξ, hexagonally packed pillars (holes) grow faster than the holes (pillars). In particular, we find that (1) Hole patterns only form when the dielectric constant of lower layer is less than the upper one. (2) With a fixed value of dielectric constant ratio, holes cannot form below a critical relative thickness h_0^* of the underlying layer.

In summary, the weakly nonlinear analysis indicates that hexagonal pattern has the largest growth rate in comparison with the stripe and square patterns at the initial stage of nonlinear growth. Depending on the dielectric contrast, initial thickness ratio between two films, and viscosities, either hexagonal-pillar or hexagonal-hole pattern can be the dominant pattern (under flat masks) that has the fastest nonlinear growth rate due to second and third order nonlinear interactions among different modes, in agreement with the experimental observations.

3 LARGE SCALE PATTERN ALIGNMENT

A significant challenge to the implementation of so-called "bottom up" approaches to patterning surfaces, via self-assembly or periodic instabilities, is the natural tendency to form multidomain structures. For example, electrohydrodynamic instabilities in thin polymer films typically generate hexagonally packed domains spanning about ten to fifteen pillars. Here we present the results of our first effort to guide these pillars into alignment over regions much greater in extent than their natural domain sizes. The key to our approach is the design of the mask. We utilize two different kinds of patterns in this realization. First, narrow protruding ridges intersect to form regular patterns on the mask and trigger the growth of pillars beneath. Those pillars under the ridges form boundaries that prevent correlation of instabilities among different domains. Later, square, triangular, or hexagonal packings of pillars that conform with the patterns of ridges develop in the regions enclosed by those ridges, and the registry is preserved from one domain to the next over a much larger area than each individual domain in unpatterned portions of the mask. The height difference of pillars beneath the ridges and those grown in between can be tuned by varying the depth of protruding ridges. Second, small square protrusions are pre-aligned into a large regular array on the mask. The polymer film on the substrate evolves into square packings of pillars under the influence of the electric field and each individual domain conforms with the mask, forming a large array of pillars. All pillars have identical heights when the spacing between individual protrusions and the annealing time are selected properly. By applying these two strategies we can achieve a large area of ordered patterns from an initially flat surface with small randomly distributed perturbations, which opens the path toward fabrications of functional polymer devices for electronic, optoelectronic, chemical, and biological applications via the electrohydrodynamic patterning.

Applying the mask of narrow ridges to the film and annealing it for several hours leaves the surface of the film patterned as shown in Figure 2. Regular rows of pillars form under ridges, and ordered triangular arrays are generated within each individual triangular domain bounded by the ridges. The low magnification optical image of Fig. 2c reveals an ordered pattern spanning over more than one hundred periods (four hundred to five hundred microns) in both the x and y directions, the largest array of packed pillars from electrohydrodynamic patterning available in the literature. The separation between the mask and substrate under the narrow protruding ridges is less than the remainder of the cross section, the locally larger electric fields lead to lower pressures beneath the ridges than in the adjacent regions, drawing in fluid that forms the first pillars. Those pillars confine the remaining unperturbed film into individual enclosures or compartments. We believe this confinement

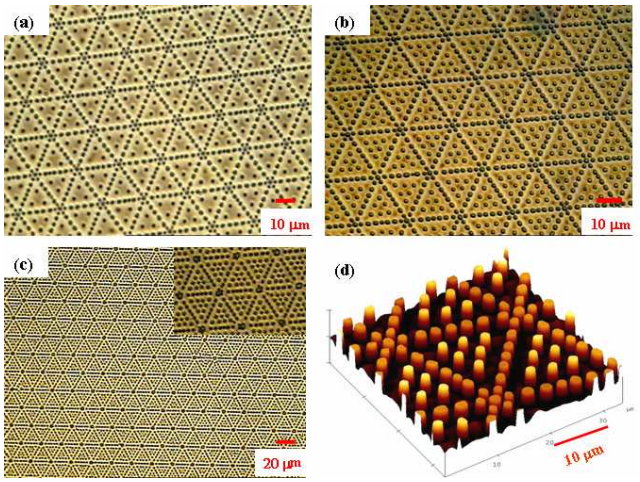

Figure 2. Optical micrographs (a, b, c) and AFM image (d) of the polymer microstructures patterned on the silicon substrate. The array contains pillars under ridges in a large triangular network within which three (a), six (b), and ten (c) triangularly packed pillars are enclosed. (d) AFM image of a typical pattern formed on the substrate with central pillars taller than those under the ridges.

to be critical to our success in achieving ordered patterns over large areas for the following reasons. When the mask is pattern-free and the initial polymer-air interface is ostensibly flat, the local perturbations in height amplify and grow into pillars once the electric field is applied. Then these initial pillars trigger the subsequent deformation of the film to produce more pillars with period λ determined by various process parameters. The size of each ordered domain is limited by a correlation length, ξ beyond which the influence of the initial nucleation becomes very weak. Therefore, the randomly distributed disturbances on the initial flat film and the finite range of the correlation prevent the formation of large scale ordered structures without guidance. Consequently, we put narrow protruding ridges on the mask to guide the pillars formed underneath and keep the spacing between boundaries large enough to allow the natural growth of pillars but smaller than the correlation length ξ, to produce uniform arrays within each unit cell.

Figure 3 shows the patterned polymer surface under a square network of narrow protruding ridges. Figure 3a and 3b demonstrate that square packing of pillars can develop both under and between ridges and the size of the central array in each unit cell can be varied by changing the spacing between patterned ridges. For example, when the spacing between ridges is 8 μm, only one pillar appears in the center of each unit cell, while a 2×2 array can be formed if the spacing increases to 12 μm. Apparently, the distance between ridges must slightly exceed $(n+1)\lambda$, where n is the number of pillars along each side, to account for the depletion of polymer adjacent to the ridges. As pillars form

under the ridges, polymer is drawn from the supply available to the interior pillars. This depletion, however, only governs the distance between the ridge and the first row of pillars inside since the spacing between the other pillars is uniform. In Fig. 3c, more than one thousand pillars are aligned into square arrays. This is particularly significant because the natural domains are hexagonal and, in this region of the sample, typically preserve their order over only seven pillars. The large magnification (inset of Fig. 3c) shows connected or partially merged pillars arising under the ridge, in which the merging of pillars into ridges is still underway.

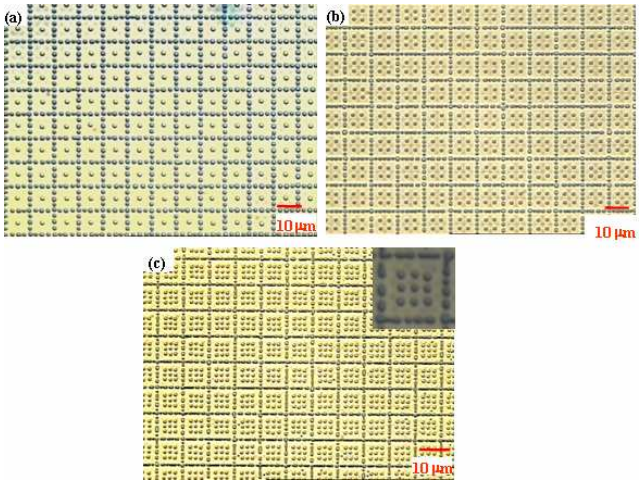

Figure 3. Optical images showing the square arrays that can be achieved under protruding ridges intersected into square networks. (a) Unit cell of one central pillar enclosed by 5×5 pillar array along ridges, spaced 8 μm apart. (b) Each unit cell consists of 2×2 array surrounded by a 6×6 array along ridges, spaced 12 μm apart. (c) 3×3 array surrounded by partially merged pillars along ridges.

As highlighted earlier, we also patterned the mask with a network of narrow trenches, by first forming regular arrays of small squares and then etching the regions between them selectively, leaving a regular array of small square protrusions with identical separations. The polymer surfaces captured by an optical microscope are shown in Fig. 4. Again, ordered arrays with various sizes form over large areas under these mask patterns. A previous study[11] indicates that polymer pillars form first under the four corners of each square protrusion, then more pillars grow inwards. Unlike with narrow ridges, the film-mask separation is larger under the narrow trenches than the square protrusions. Therefore, all pillars have identical heights if the annealing time is too short for pillars to form under the trenches, as shown in Fig. 4(d). This makes trenches preferable to ridges if identical pillar heights are required. Since the intrinsic pattern is hexagonal under a flat mask, it is understandable that the order deteriorates slightly for larger unit cells, e.g. a 4×4 array (in Fig. 4c). It should be noted that this deterioration is due to processes within the unit cell, not interactions between them.

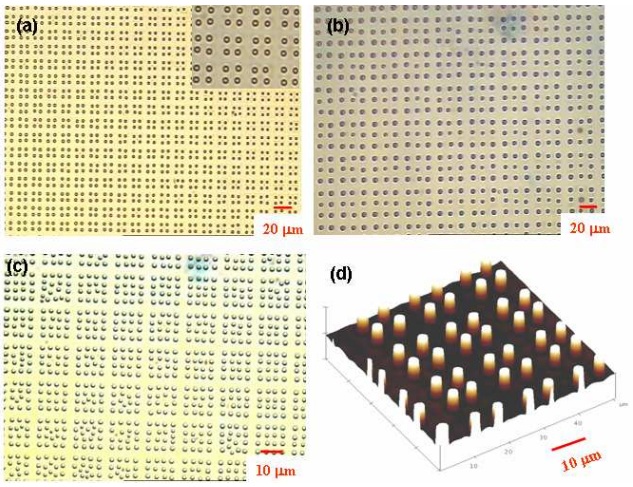

Figure 4. Optical images of the polymer patterns [(a) 2×2, (b) 3×3, and (c) 4×4 arrays] formed under the mask consisting of small square protrusions separated with identical distances. (d) AFM image of a typical 2×2 array on the substrate. All pillars have the identical heights.

In summary, our results have important implications for the capability and versatility in electrohydrodynamic patterning of thin polymer films over large areas, as compared with its natural domain size. We have demonstrated that proper design of the mask, i.e. both narrow ridges and trenches on a patterned mask can guide development of pillars at desired locations. This effort in enabling large-scale assembly of thin polymer films via electrohydrodynamic patterning opens the path toward applications requiring larger areas of well arrayed patterning.

REFERENCES

[1] Chou, S. Y.; Zhuang, L. J. Vac. Sci. Technol. B. 17, 3197, 1999.
[2] Schäffer, E.; Thurn-Albrecht T.; Russell T. P.; Steiner U. Nature. 403, 874, 2000.
[3] Schäffer, E.; Thurn-Albrecht T.; Russell T. P.; Steiner U. Europhys. Lett. 53, 518, 2001.
[4] Pease, L. F.; Russel W. B. J. Non-Newton. Fluid. Mech. 102, 233, 2002.
[5] Fermigier, M.; Limat, L.; Wesfreid, J. E.; Boudinet, P.; Quilliet, C. J. Fluid. Mech. 236, 349, 1992.
[6] Wu N.; Pease, L. F.; Russel W. B. Langmuir. 21, 12290, 2005.
[7] Lin, Z.; Kerle, T.; Russell, T. P. Macromolecules. 35, 3971. 2002.